Ultrasonic properties near 50 K of the quasi-one-dimensional conductors $A_{0.30}MoO_3$ (A = K, Rb) and $Rb_{0.30}(Mo_{1-x}V_x)O_3$



2009 J. Phys.: Condens. Matter 21 215603

(http://iopscience.iop.org/0953-8984/21/21/215603)

J. Phys.: Condens. Matter **21** (2009) 215603 (7pp) doi:10.1088/0953-8984/21/21/215603

# Ultrasonic properties near 50 K of the quasi-one-dimensional conductors $A_{0.30}MoO_3$ (A = K, Rb) and $Rb_{0.30}(Mo_{1-x}V_x)O_3$

**M Saint-Paul, J Dumas and J Marcus**

Institut Néel, CNRS/UJF, BP 166, F-38042 Grenoble Cedex 9, France

E-mail: jean.f.dumas@grenoble.cnrs.fr

Received 11 March 2009, in final form 31 March 2009
Published 24 April 2009
Online at stacks.iop.org/JPhysCM/21/215603

**Abstract**

The charge density wave (CDW) nonlinear conductivity of the blue bronzes $A_{0.30}MoO_3$ (A = K, Rb) shows two different regimes depending on the temperature: a strongly damped CDW motion above ~50 K and a CDW motion with almost no damping below ~50 K. In a search for an elastic signature of this CDW behaviour, we performed ultrasonic measurements on $A_{0.30}MoO_3$ single crystals in the temperature range 4–300 K. In $Rb_{0.30}MoO_3$, at $T \sim 50$ K, upon cooling, a large increase of the sound velocity for the longitudinal mode measured along the $[\bar{2}01]$, [102] and $b$ directions is observed. The ultrasonic attenuation coefficient shows an increase down to 50 K followed by a plateau. Similar results are found in $K_{0.30}MoO_3$. In V-doped samples, $Rb_{0.30}(Mo_{1-x}V_x)O_3$ ($x = 0.4\%$) the anomaly broadens and is shifted towards higher temperatures. The results are discussed in relation to the changes in the CDW rigidity, disorder and dielectric response. A scenario based on a glass transition for the CDW superstructure is proposed.

(Some figures in this article are in colour only in the electronic version)

## 1. Introduction

The so-called blue bronzes with the formula $A_{0.30}MoO_3$ (A = K, Rb) are at room temperature quasi-one-dimensional conductors that undergo a Peierls transition at 183 K towards an incommensurate semiconducting charge density wave (CDW) ground state [1, 2]. In the CDW state, a periodic lattice distortion is accompanied by a modulation of the electron density:

$$\rho = \rho_0 + \rho_1 \cos[2k_F x + \phi(x)]$$

where $k_F$ denotes the Fermi wavevector, and $\rho_1$ and $\phi$ the amplitude and the phase of the CDW with respect to the undistorted lattice.

The CDW wavevector approaches the commensurate value $0.75b^*$ as the temperature is decreased below approximately 100 K. At low electric field, the collective CDW mode is pinned to the lattice by randomly distributed impurities. The CDW can overcome the pinning forces of the impurities when a small electric field greater than a threshold value is applied, leading to a remarkably rapid rise of the conductivity with field. Depending on the temperature, two qualitatively different regimes have been found for the CDW dynamics [3, 4]: above ~50 K, the nonlinear conductivity above a small depinning threshold field (~10–100 mV cm$^{-1}$) arises from a deformable CDW with strong damping by normal carriers; below ~50 K, the CDW dynamics, in the insulating state, is essentially that of a rigid body with a very small damping above an abrupt large threshold field (~10 V cm$^{-1}$). This change in the CDW rigidity is accompanied by anomalies in a large number of properties such as: low frequency dielectric response [5–9], thermally stimulated depolarization current [5, 10], unit cell parameters [11], proton channelling [12] and EPR intensity of $Mo^{5+}$ lines [13]. No structural phase transition occurs at ~50 K.

In V-doped blue bronzes, the Peierls transition is broadened towards a disordered state characterized by a short

 

range CDW order [14, 15]. V ions are non-isoelectronic impurities which act as strong pinning centres. $V^{5+}$ vanadium ions are substituted for $Mo^{6+}$ ions. The threshold field for CDW depinning is larger than in pure samples, $E_t \sim 1$ V cm$^{-1}$ at 77 K [15].

In order to obtain additional information on the nature of the change in the CDW state near 50 K, we performed ultrasonic measurements on single crystals of $A_{0.30}MoO_3$ (A = K, Rb) and $Rb_{0.30}Mo_{1-x}V_xO_3$ in the temperature range 4–300 K. Previous ultrasonic experiments on $K_{0.30}MoO_3$ were limited to a temperature range near the Peierls transition [16]. The anomalies in the elastic constants were related to those in the specific heat [16, 17]. We have reported recently some ultrasonic measurements in $Rb_{0.30}MoO_3$ [18]. We discuss our results in relation to the changes in the CDW elasticity, disorder and dielectric response. A scenario based on a glass transition for the CDW superstructure is proposed. The blue bronze crystal structure has a face-centred monoclinic structure with space group $C2/m$. It consists of clusters of ten $MoO_6$ octahedra arranged in chains along the [010] direction, the high conductivity $b$ axis of the monoclinic unit cell. The chains are bonded in sheets along the [102] direction and separated by the alkaline ions, so that the crystals can be easily cleaved along the $(\bar{2}01)$ plane. This structural anisotropy results in an anisotropy of the stiffness of the system: neutron measurements of the sound velocity [19] show a decreasing stiffness from the $b$ to the $a + 2c$ then to the $2a^* - c^*$ (perpendicular to the $MoO_6$ octahedra layers) directions.

## 2. Experimental results

The pure and V-doped blue bronze single crystals have been prepared by standard electrocrystallization. The vanadium concentration was obtained by microprobe analysis. The samples appear as platelets parallel to the cleavage plane with $b$ as the long direction. The typical dimensions of the crystals used in this study after cleavage were: $5 \times 4 \times 2$ mm$^3$ for $Rb_{0.30}MoO_3$, $3 \times 2 \times 0.1$ mm$^3$ for $K_{0.30}MoO_3$ and $4 \times 3 \times 0.2$ mm$^3$ for $Rb_{0.30}Mo_{1-x}V_xO_3$, corresponding to the $b$ axis, [102] and $[\bar{2}01]$ directions, respectively. Because of the existence of a large number (13) of independent elastic constants related to the monoclinic symmetry in the elasticity tensor, elastic measurements were performed only with three longitudinal modes. The sound velocity of the longitudinal modes was measured at 15 MHz by the standard pulse echo technique with $LiNbO_3$ transducers [16]. The transducers were attached to the crystal by means of Apiezon grease. Because of the high ultrasonic attenuation, difficulties have been found to generate longitudinal modes at higher frequencies. A resonant method was used in the [102] direction in $Rb_{0.30}MoO_3$ at an excitation frequency of about 1 MHz close to the resonance frequency of the sample and far below the resonant frequency of the transducer. The temperature was varied at a slow rate, less than 1 K min$^{-1}$.

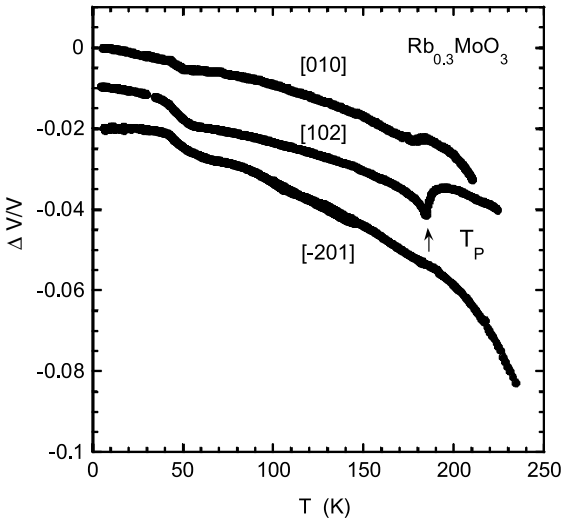


**Figure 1.** Relative change of the velocity of the longitudinal mode along the $[\bar{2}01]$, [102] and [010] $\parallel b$ directions as a function of temperature for $Rb_{0.30}MoO_3$ at 15 MHz. Curves are shifted vertically for clarity (from [18]). For each curve, the velocity variation is relative to its value at 4.2 K.

### 2.1. $Rb_{0.30}MoO_3$

The relative change of the velocity $\Delta V/V = (V - V_0)/V_0$ of the longitudinal mode generated along the $[\bar{2}01]$, [102] and $b$ directions in $Rb_{0.30}MoO_3$ measured at 15 MHz is shown in figure 1. The longitudinal mode along the [102] direction exhibits a pronounced softening at the Peierls transition, in agreement with our previous work on $K_{0.30}MoO_3$ [16] and with Young's modulus measurements [17, 20]. Clearly, the longitudinal modes exhibit a large stiffening when the temperature decreases below ~50 K. One should note that a change of the velocity is observed for the three directions while the change at the Peierls transition is observed mainly for the [102] direction.

The longitudinal sound velocities obtained at 300 K along the $b$ axis, [102] and $[\bar{2}01]$ directions are, respectively, 5300, 4800 and 3300 m s$^{-1}$. The corresponding elastic stiffness constants $C_{22} = 1.2 \times 10^{11}$ N m$^{-2}$, $C_{\parallel} = 10^{11}$ N m$^{-2}$ and $C_{\perp} = 4.6 \times 10^{10}$ N m$^{-2}$ were deduced from the sound velocity results at 15 MHz with the density $\rho = 4.3$ g cm$^{-3}$.

In figure 2, we present the low temperature dependence of the longitudinal mode measured along the [102] direction at 15 MHz together with the attenuation coefficient. The attenuation shows an increase down to ~50 K and then remains roughly constant.

The relative change of the velocity of the longitudinal mode and the attenuation coefficient measured along the transverse $[\bar{2}01]$ direction are shown in figure 3. The attenuation shows a behaviour similar to that observed in the [102] direction.

In figure 4, we compare the relative changes of the velocity of the longitudinal mode along the [102] direction and the changes in the attenuation measured at the two frequencies 15 and 1 MHz. The onset of the anomaly at 1 MHz is clearly shifted towards lower temperatures.

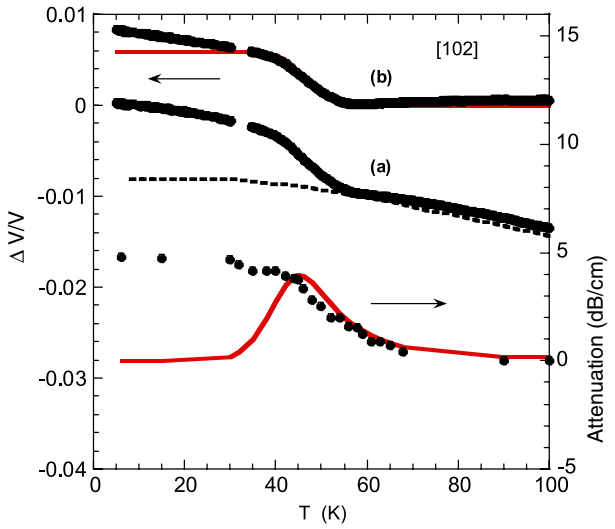


**Figure 2.** Left scale: low temperature dependence of the velocity of the longitudinal mode along the [102] direction at 15 MHz for $Rb_{0.30}MoO_3$. Right scale: attenuation as a function of temperature. Dotted line: anharmonic contribution evaluated with an effective Grüneisen $\gamma = 3$. The solid lines are obtained with equation (2) and (3) and a time constant $\tau = 10^{-11}\exp(325/T)$. See the text. (a) Our results; (b) temperature dependence when the background contribution is subtracted.

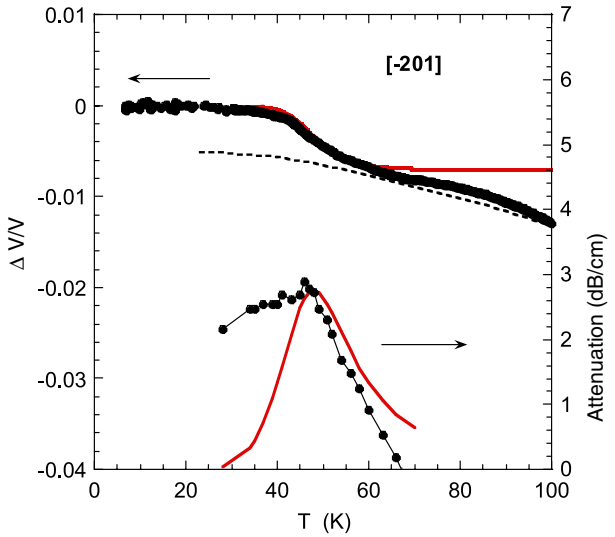


**Figure 3.** Relative change of the velocity of the longitudinal mode propagating along the [$\bar{2}$01] direction as a function of temperature at 15 MHz for $Rb_{0.30}MoO_3$. Dotted line: anharmonic contribution evaluated with an effective Grüneisen parameter $\gamma = 3.6$. The solid lines are obtained with equations (2) and (3) with the relaxation time $\tau = 10^{-11}\exp(325/T)$. See the text.

### 2.2. $K_{0.30}MoO_3$

In figure 5, we show the relative change of the sound velocity for the longitudinal mode along [102] for a $K_{0.30}MoO_3$ crystal measured at 15 MHz as well as the attenuation.

A step-like increase is also observed below 50 K. The temperature dependence of the attenuation amplitude is very similar to that found in $Rb_{0.30}MoO_3$. These results indicate that the alkaline atoms play no major role in the ultrasonic properties.

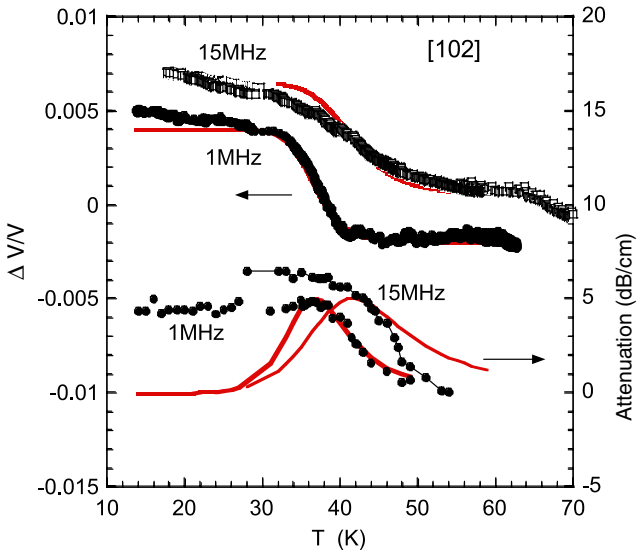


**Figure 4.** Left scale: low temperature dependence of the velocity of the longitudinal mode along the [102] direction for $Rb_{0.30}MoO_3$ measured at 15 and 1 MHz in the same experimental run. The anharmonic contribution was subtracted. The two upper curves have been shifted vertically for clarity. Right scale: attenuation as a function of temperature. The attenuation measured at 1 MHz was multiplied by 15. Solid lines are calculated with equations (2) and (3) with the relaxation times $\tau = 10^{-11}\exp(325/T)$ at 15 MHz and $\tau = 10^{-11}\exp(360/T)$ at 1 MHz. Linear temperature dependence below 30 K: $A = 0.6 \times 10^{-4}$ K$^{-1}$ and $A = 0.2 \times 10^{-4}$ at 15 MHz and 1 MHz, respectively. See the text.

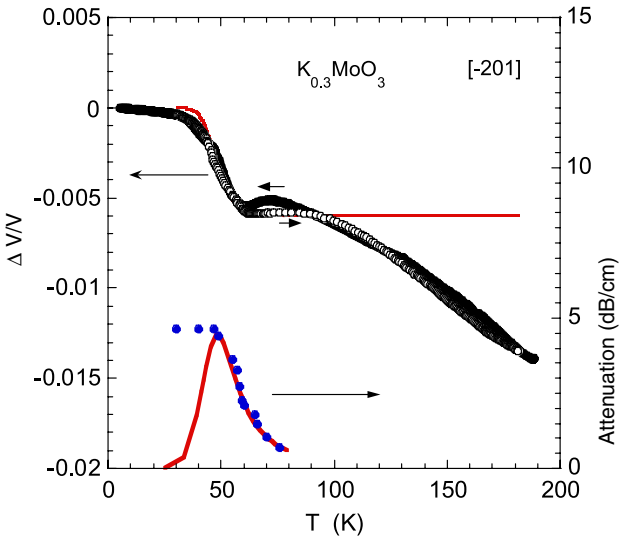


**Figure 5.** Left scale: relative change of the velocity of the longitudinal mode propagating along the [$\bar{2}$01] direction as a function of temperature at 15 MHz for $K_{0.30}MoO_3$. Right scale: attenuation as a function of temperature. The solid lines are obtained with equations (2) and (3) with the relaxation time $\tau = 10^{-11}\exp(325/T)$.

The sound velocities for the longitudinal modes measured at 300 K are 4500 m s$^{-1}$ along $b$ and 3100 m s$^{-1}$ along

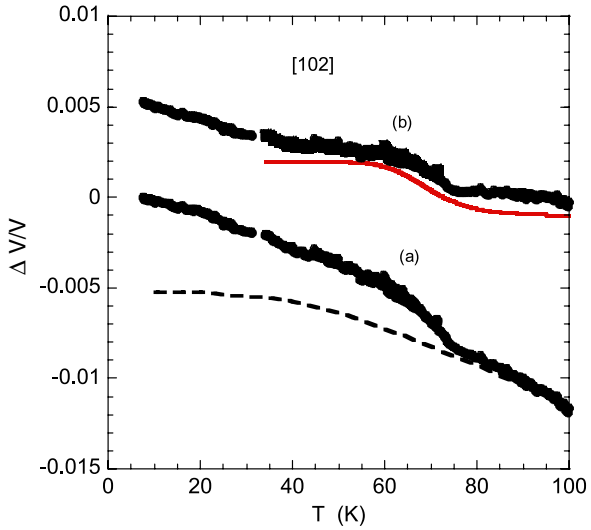


**Figure 6.** Relative change of the velocity of the longitudinal mode propagating along the [102] direction as a function of temperature at 15 MHz for $Rb_{0.30}Mo_{1-x}V_xO_3$, $x = 0.4$ at.%. (a) Our results. Dashed line: anharmonic contribution (equation (1)) evaluated with an effective Grüneisen parameter $\gamma = 3$. (b) Excess change in $\Delta V/V$ after subtracting the Debye background. Solid lines: fit according to equation (1) with $E_a = 500$ K. See the text.

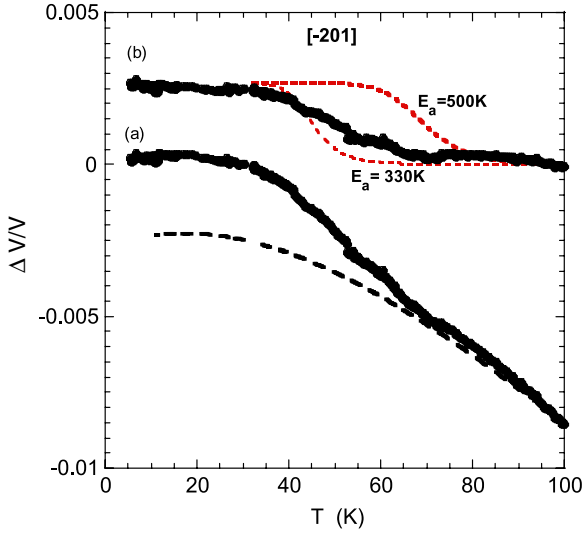


**Figure 7.** As in figure 6, but for the [$\bar{2}$01] direction. Grüneisen parameter $\gamma = 3.6$.

[102]. The corresponding elastic constants are $C_{22} = 0.87 \times 10^{11}$ N m$^{-2}$ and $C_{\parallel} = 0.4 \times 10^{11}$ N m$^{-2}$.

### *2.3. V-doped blue bronze $Rb_{0.30}Mo_{1-x}V_xO_3$*

In order to study the role of structural disorder, we performed ultrasonic measurements on a crystal $Rb_{0.30}Mo_{1-x}V_xO_3$, $x = 0.4$ at.%. V atoms are substituted for the molybdenum atoms. They are non-isoelectronic impurities which act as strong pinning centres for the CDW. Only short range CDW order is found [14]. In figures 6 and 7 we show the temperature dependence of the velocity of the longitudinal mode along the [102] and [$\bar{2}$01] directions, respectively, measured at 15 MHz. Along the [102] direction, we notice that the anomaly of the velocity seems to occur at a temperature $T \sim 70$ K higher than that found for the undoped samples. The anomaly along the [$\bar{2}$01] direction shows a broadening and its amplitude is smaller than that observed along the [102] direction. The onset temperature of the anomaly is also higher than in undoped samples.

## 3. Discussion

We now discuss the anomalous behaviour of the ultrasonic properties. The normal behaviour is a gradual increase of the sound velocity with decreasing temperature. Since no structural phase transition occurs at $T \sim 50$ K one can rule out such an effect to explain the observed anomalies. Another possible mechanism could be a change in the bonding due to a change in the electronic energy band structure with temperature. This would also lead to a change in the modulation wavevector which is not observed [1, 23].

The increase of the sound velocity upon cooling can be described by the anharmonicity of the lattice vibrations. The temperature dependence of the elastic constant due to the lattice anharmonicity, in an isotropic approximation, is predicted to be proportional to the total phonon energy density [21]. In the formulation of Maris [21], which takes into account the perturbation due to the measuring wave on the phonon distribution function, the temperature dependence for the adiabatic sound velocity may be written in terms of the Debye model as

$$\frac{\Delta V}{V_0} = -\frac{\gamma^2 C(T)}{2\rho V_0^2} T \qquad (1)$$

where $V_0$ is the value of the sound velocity at the lowest temperature, $\rho$ is the mass density, $\gamma$ is the effective Grüneisen parameter which describes the anharmonic coupling of the external strain to the thermal phonon modes and $C(T)$ is the Debye specific heat characterized by a Debye temperature of 320 K [22] for $Rb_{0.30}MoO_3$. Equation (1) gives a linear temperature dependence at high temperatures and a $T^4$ temperature dependence at the lowest temperatures. Equation (1) provides a good fit to the data above 50 K, but large discrepancies are found below 50 K as can be seen in figures 2 and 3.

The large relative change in $\frac{\Delta V}{V_0}$ near 50 K corresponds therefore to a stiffening of the elastic constant. This effect is very likely related to the loss of screening of the CDW as the concentration of normal carriers becomes vanishingly small at low temperature. This mechanism stiffens the CDW and leads to an increase of the longitudinal phason velocity which has been observed by neutron scattering [23].

This descreening may be responsible for the weak increase of the lattice parameter $b$ upon cooling below 50 K and for a nearly temperature-independent behaviour for the interlayer distance $d_{[\bar{2}01]}$ [11].

We analyse the observed stiffening of the elastic constants in terms of a relaxational process characterized by one

relaxation time $\tau$. The sound velocity and attenuation are related to the measurement frequency $\omega$ (15 or 1 MHz) and time constant $\tau$ by [21]

$$\frac{\Delta V}{V_0} = \frac{(V_u - V_R)}{2V_R} \frac{(\omega\tau)^2}{1+(\omega\tau)^2} \quad (2)$$

and

$$\alpha = \frac{1}{4} \frac{(V_u - V_R)}{V_R^2} \frac{\omega^2\tau}{1+(\omega\tau)^2} \quad (3)$$

where $V_u$ and $V_R$ are the unrelaxed and relaxed sound velocity. In this picture, the maximum in the attenuation occurs at a temperature where the condition $\omega\tau = 1$ is fulfilled.

We tried to fit the data with a thermally activated mechanism for $\tau$ characterized by an activation energy $E_a$, $\tau = \tau_0 \exp(E_a/T)$. After subtracting the anharmonic contribution, a good fit for the longitudinal modes is shown in figure 4 taking an activation energy $E_a = 335$ K for the data obtained at 15 MHz and 360 K for the data at 1 MHz and $\tau_0 \sim 10^{-11}$ s.

At low temperatures $T < 30$ K, the excess contribution shows a linear temperature dependence which cannot be related to equation (2). See figures 2 and 4.

It should be noted that a similar activation energy value $E_a = 325$ K characterizes the so-called low temperature slow relaxational $\beta$ process observed in the dielectric measurements and becomes dominant below a freezing temperature $T_g \sim 23$ K [5]. Nevertheless, the elastic pre-exponential factor $\tau_0 \sim 10^{-11}$ s is two orders of magnitude smaller than the dielectric pre-exponential factor $\tau_0 \sim 10^{-9}$ s [5].

In glassy systems, the sound velocity exhibits a frequency-dependent step-like stiffening near the glassy transition [24]. In the transition region, the sound velocities show a pronounced variation between their respective low frequency and high frequency limits. This is related to a slowing down of the stress relaxation. In general, the relaxation mechanism cannot be described by a single relaxation time.

Since the $MoO_6$ layers are separated by alkaline ions, one may expect that they are involved in the ultrasonic velocity in the transverse direction and that structural rearrangements around alkaline atoms occur. However, a very similar activation energy $E_a \sim 330$ K and relaxation time $\tau_0$ are found in $K_{0.30}MoO_3$. Surprisingly, there is no important role of the alkaline element.

Since the attenuation $\alpha$ is mainly due to interactions between the ultrasonic wave and lattice vibrations, the conventional behaviour is a maximum followed by a decrease at low temperature. The observed additional contribution at low temperature characterized by a plateau indicates that there is a wide distribution of relaxation times. We ascribe the plateau to a disorder in the CDW superlattice.

In $Rb_{0.30}Mo_{1-x}V_xO_3$, using the same procedure, we obtain an activation energy $E_a$ of approximately 500 K for the [102] direction. For the [$\bar{2}$01] transverse direction, the thickness of the sample is about 0.1 mm which limits experimental accuracy. However, an activation energy 330 K $< E_a <$ 500 K can be estimated. See figure 7.

In this context, we tried a fit with the widely used Vogel–Fulcher law: $\tau = \tau_0 \exp[U/(T - T_0)]$, valid for $T > T_0$. In this formula, $\tau_0$ represents the inverse attempt frequency, $U$ is the average activation energy and $T_0$ is the freezing temperature. In this picture, relaxation times are related to a distribution of activation energies with the freezing temperature $T_0$. The Vogel–Fulcher law describes satisfactorily the glass-like behaviour in the dielectric response of the blue bronzes [7, 8] and similarly ferroelectric relaxors for which a random distribution of electric fields prevent the onset of the long range ferroelectric order [25]. The elastic strain couples quadratically to the order parameter which corresponds to the spontaneous electric polarization, in the ordered ferroelectric phase [26]. The onset of a local polarization in small volumes and having a random orientation in space are induced by the local lattice dynamics involving soft phonons [27]. However, in the blue bronzes the order parameter is nearly constant below ∼77 K [1]; a mechanism based on a biquadratic coupling between the strain and the order parameter is not expected to give a rapid rise of the velocity with temperature. Nevertheless, the CDW phase fluctuations (phasons) induce charge fluctuations and hence couple to longitudinal acoustic phonons [28]. The acoustic elastic mode is coupled to the square of the long range Coulomb interaction. The change in the phason behaviour observed around 40 K [23] could be related to the ultrasonic anomalies observed in the same temperature range. Theories [28] predict that at very low temperatures the acoustic-like phason mode turns into an optical mode.

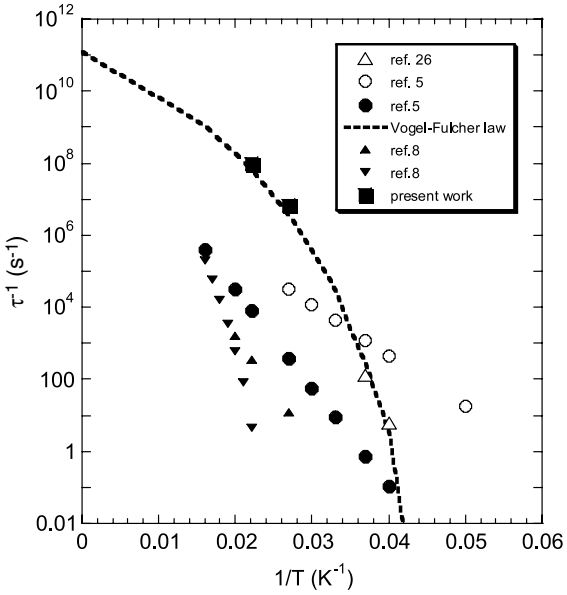


**Figure 8.** Frequency (log scale) as a function of reciprocal temperature of the ultrasonic maximum ($\omega\tau = 1$) in $Rb_{0.30}MoO_3$ (■). (●, ○): maximum in the real part of the dielectric constant (from [5]); (▲, ▼) from [8]. (△) Maximum in the thermoelectric power, from [29]. Dotted line: Vogel–Fulcher law: $\omega = 10^{11} \exp(-220/(T - 16))$.

In figure 8, we have tentatively plotted the inverse of the temperature in the maximum of the ultrasonic attenuation for the two frequencies 15 and 1 MHz together with the maximum in the low-frequency-dependent thermoelectric power [29]. Some of the data resulting from measurements of the real part

of the dielectric constant [5, 8] have also been included. More frequencies would be necessary to draw firm conclusions. However, a fit of the data is obtained with the parameters $U = 220$ K, $T_0 = 16$ K and $\tau_0 = 10^{-11}$ s. This seems to be consistent with a glassy-like state at low temperature for the CDW with frozen domains.

A common feature of glasses above liquid helium temperature is a linear decrease with increasing temperature of the fractional change of the sound velocity. This feature is known as the Bellessa effect and has been reported for a large number of disordered solids [30, 31]: $\Delta V/V_0 = -AT$.

Both anharmonic and tunnelling activation processes contribute to this linear temperature dependence. The corrections to the sound velocity due to the coupling of the sound wave with unspecified low energy vibrational modes have been examined [30, 31]. A general behaviour has been found: the coefficient $A$ is found to be inversely proportional to the elastic stiffness $\rho V^2$. Exceptions to this trend are the silica-based glasses. The value of the temperature coefficient $A \sim 0.2 \times 10^{-4}$ K$^{-1}$ at 1 MHz and $\sim 0.6 \times 10^{-4}$ K$^{-1}$ at 15 MHz found for the [102] direction (see figure 4), together with $\rho V^2 = 10^{11}$ N m$^{-2}$, corroborate the data shown in figure 2 in [31] for disordered and amorphous materials. In V-doped samples, a linear term is also found with $A \sim 0.7 \times 10^{-4}$ K$^{-1}$. In this context, the anomaly at ~50 K in the ultrasonic properties corresponds to a transition towards a glassy state for the CDW sublattice.

The CDW glassy-like state results from interactions of the CDW with randomly distributed impurities which destroy the long range phase coherence. These interactions lead to the formation of CDW domains which would also be responsible for the strong increase below ~40 K in the anisotropic backscattering yield in proton channelling experiments [12]. This increase was found to be too large to be accounted for by point lattice defects. On the other hand, very low temperature specific heat measurements accompanied by time-dependent effects have revealed low energy excitations due to the disordered nature of the CDW ground state [32].

In this context, the plateau observed below ~50 K in the temperature dependence of the attenuation is attributed to disorder in the CDW sublattice in a structurally ordered host crystal.

In V-doped crystals the size of domains of coherence of CDW is smaller since it is inversely proportional to the impurity concentration. The structural disorder leads to a broadening of the Peierls transition [14] and also a smearing out of the anomaly at ~60 K. Since the domain size decreases upon doping, the density of normal carriers necessary to screen the CDW phase deformations increases. Therefore, the onset of the anomaly is shifted towards higher temperature. A similar scenario was proposed by Biljakovic *et al* [6] for the glass transition in doped $TaS_3$ CDW compounds.

From the above results, we propose that the anomaly near 50 K is essentially a dynamic freezing process rather than a thermodynamic phase transition. The existence of the linear term $AT$ at $T < 30$ K corroborates the description in terms of CDW sublattice glass.

## 4. Conclusion

In summary, the present ultrasonic measurements represent a sensitive probe of the pronounced anomaly at $T \sim 50$ K. They reveal an important stiffening of the longitudinal elastic constants $C_{22}$, $C_{\parallel}$ and $C_{\perp}$ defined along the $b$, [102] and [$\bar{2}$01] directions in the temperature range 4–50 K in $Rb_{0.30}MoO_3$ as well as in $K_{0.30}MoO_3$. The anomaly in the elastic constants is accompanied by an increase of the attenuation followed by a plateau. In V-doped samples where the CDW coherence length is shorter, the anomaly is broadened and shifted towards higher temperature. The results have been discussed in terms of relaxation behaviour whose nature is not completely understood.

The microscopic nature of structural states cannot be deduced from ultrasonic measurements. These states are attributed to the presence of CDW domains. The anomaly is very likely a dynamic effect rather than a thermodynamic phase transition. The data corroborate the description in terms of a CDW glass resulting from the competition between elasticity and disorder. It would now be interesting to investigate the remarkable CDW glassy properties by elastic measurements at lower frequencies.

## Acknowledgments

The authors are grateful to J Brill and K Biljakovic for helpful discussions.

## References

[1] See in Schlenker C (ed) 1989 *Low Dimensional Electronic Properties of Molybdenum Bronzes and Oxides* vol 11 (Dordrecht: Kluwer)
[2] See in Schlenker C, Dumas J, Greenblatt M and van Smaalen S (ed) 1996 *Physics and Chemistry of Low Dimensional Inorganic Conductors* (*NATO-ASI Series B* vol 354) (New York: Plenum)
[3] Mihaly G and Beauchène P 1987 *Solid State Commun.* **63** 911
Mihaly G, Beauchène P, Marcus J, Dumas J and Schlenker C 1988 *Phys. Rev.* B **37** 1047
Schlenker C, Dumas J, Escribe-Filippini C and Boujida M 1989 *Phys. Scr.* T **29** 55
[4] Fleming R M, Cava R J, Schneemeyer L F, Rietman E A and Dunn R G 1986 *Phys. Rev.* B **33** 5450
[5] Staresinic D, Hosseini K, Brütting W, Biljakovic K, Riedel E and van Smaalen S 2004 *Phys. Rev.* B **69** 113102
Staresinic D, Zaitsev-Zotov S V, Baklanov N I and Biljakovic K 2008 *J. Chem. Phys.* **128** 094501
[6] Biljakovic K, Staresinic D and Dominko D 2009 *Physica* B **404** 456
[7] Ya Nad F and Monceau P 1993 *J. Physique* IV **3** 343
Ya Nad F and Monceau P 1993 *Solid State Commun.* **87** 13
[8] Zawilsky B, Klein T and Marcus J 2002 *Solid State Commun.* **124** 39
[9] Yang J and Ong N P 1991 *Phys. Rev.* B **44** 7912
[10] Cava R J, Fleming R M, Rietman E A, Dunn R G and Schneemeyer L F 1984 *Phys. Rev. Lett.* **53** 1677
[11] Tian M, Chen L and Zhang Y 2000 *Phys. Rev.* B **62** 1504
[12] Dumas J, Arbaoui A, Daudin B, Dubus M, Lopes E and Band M A 1991 *Synth. Met.* **41–43** 3813
[13] Dumas J, Laayadi B and Buder R 1989 *Phys. Rev.* B **40** 10088
Dumas J, Laayadi B and Buder R 1989 *Solid State Commun.* **72** 429

[14] Ravy S, Rouzière S, Pouget J P, Brazovskii S, Marcus J, Bérar J F and Elkaim E 2006 *Phys. Rev.* B **74** 174102
[15] Girault S 1987 *Thesis* Université Paris Sud
[16] Saint-Paul M and Tessema G X 1989 *Phys. Rev.* B **39** 8736
[17] Brill J W, Chung M, Kuo Y K, Zhan X, Figueroa E and Mozurkewich G 1995 *Phys. Rev. Lett.* **74** 1182
[18] Saint-Paul M, Dumas J and Marcus J 2009 *Physica* B **404** 430
[19] Pouget J P, Hennion B, Escribe-Filippini C and Sato M 1991 *Phys. Rev.* B **43** 8421
[20] Bourne L C and Zettl A 1986 *Solid State Commun.* **60** 789
[21] Maris H J 1971 *Physical Acoustics* vol VII, ed W P Mason (New York: Academic) p 279
[22] See in Schlenker C (ed) 1989 *Low Dimensional Electronic Properties of Molybdenum Bronzes and Oxides* vol 11 (Dordrecht: Kluwer) p 177
[23] Ravy S, Requardt H, Le Bolloc'h D, Foury-Leylekian P, Pouget J P, Currat R, Monceau P and Krisch M 2004 *Phys. Rev.* B **69** 115113
Hennion B, Pouget J P and Sato M 1992 *Phys. Rev. Lett.* **68** 2374
[24] Jäckle J 1986 *Rep. Prog. Phys.* **49** 171
[25] Pirc R and Blinc R 2007 *Phys. Rev.* B **76** 020101
Kutnjak Z, Filipic C, Levstik A and Pirc R 1993 *Phys. Rev. Lett.* **70** 4015
[26] Lüthi B 2005 *Physical Acoustics in the Solid State* (*Springer Series in Solid State Sciences* vol 148) (Berlin: Springer)
[27] Dmowski W, Vakhrushev S B, Jeong I-K, Hehlen M P, Trouw F and Egami T 2008 *Phys. Rev. Lett.* **100** 137602
[28] Nakane Y and Takada S 1986 *J. Phys. Soc. Japan* **55** 2235
[29] Kriza G, Mihaly G and Gruner G 1989 *Phys. Rev. Lett.* **62** 2032
[30] Bellessa G 1978 *Phys. Rev. Lett.* **40** 1456
[31] Nava R 1994 *Phys. Rev.* B **49** 4295
[32] Odin J, Lasjaunias J C, Biljakovic K, Hasselbach K and Monceau P 2001 *Eur. Phys. J.* B **24** 315
Dahlhauser K J, Anderson A C and Mozurkewich G 1986 *Phys. Rev.* B **34** 4432